IEEE Photonics Journal
An IEEE Photonics Society Publication

Design of High Sensitive Pressure and Temperature Sensor Using Photonic Crystal Fiber for Downhole Application

Volume 4, Number 5, October 2012

S. Padidar
V. Ahmadi, Senior Member, IEEE
M. Ebnali-Heidari, Member, IEEE

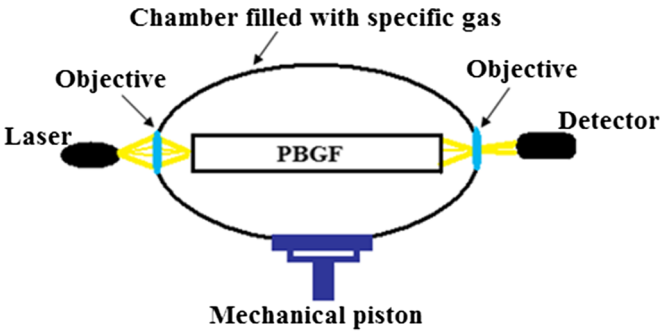

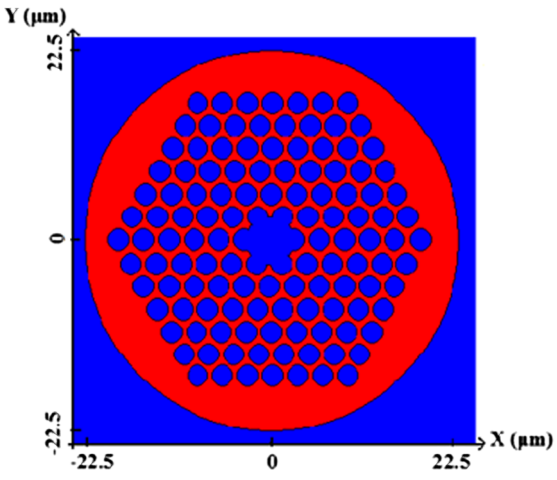

DOI: 10.1109/JPHOT.2012.2212242
1943-0655/$31.00 ©2012 IEEE

Design of High Sensitive Pressure and Temperature Sensor Using Photonic Crystal Fiber for Downhole Application

S. Padidar,[1] V. Ahmadi,[1] *Senior Member, IEEE*, and M. Ebnali-Heidari,[2] *Member, IEEE*

[1]Department of Electrical and Computer Engineering, Tarbiat Modares University, Tehran, Iran
[2]Faculty of Engineering, University of Shahrekord, Shahrekord, Iran

DOI: 10.1109/JPHOT.2012.2212242
1943-0655/$31.00 ©2012 IEEE

Manuscript received June 29, 2012; revised July 28, 2012; accepted August 1, 2012. Date of publication August 8, 2012; date of current version August 17, 2012. Corresponding author: V. Ahmadi (e-mail: v_ahmadi@modares.ac.ir).

Abstract: Permanent monitoring of two important parameters, pressure and temperature, plays an important role in reservoir engineering to increase the production rates of oil wells. The numerous advantages of photonic crystal fiber (PCF) sensors make them a proper choice as a sensor in the hostile environment of well. In this paper, we propose short length, high sensitive pressure, and temperature sensor based on hollow-core PCF. The validation of the proposed design is carried out by employing the 3-D finite-difference time domain (FDTD) method. Our sensor mechanism is based on the transmission peak wavelength shift caused by the temperature/pressure changes, with special emphasis on geometric parameters of the structure of PCF. We show that the proposed design provides a sensitivity about 480 nm/RIU with a linear dependence of the resonance wavelength on the refractive index of the ambient and PCF holes at $\lambda = 1.55$ μm.

Index Terms: Engineered photonic, sensors, fiber optics systems.

1. Introduction

There is a great interest in real-time acquisition data in reservoir engineering. Accurate, reliable, frequent, and real-time measurements of physical quantities such as pressure, temperature, strain, and flow are known to be of great importance for downhole monitoring, which helps to optimize the production rates and reservoir recovery [1], [2]. Pressure and temperature of the wells are crucial parameters in reservoir management. Typical amount of pressure and temperature in oil wells are 138 MPa (20 kpsi) and 175 °C, respectively [3].

Conventional electrical gauges used for in-well parameter measurement have a high failure rate in a high temperature environment. They have a lifetime of 1–3 years in limited temperature up to 175 °C [3]. Therefore, they are not appropriate for downhole application with temperature over 200 °C.

Optical fiber sensors have well known advantages over their electrical counterparts, such as small size, light weight, electromagnetic immunity, and high resistance to corrosion. They have an estimated lifetime of 5–10 years and function up to 250 °C. So, optical fiber sensors for downhole application have attracted great interest for a variety of technological applications [4]. These new sensors have been used in different oil fields, and their proper sensitivity and long life time have been proven practically. For example, in 1993–2002, pressure, temperature, and flow rate sensors have been installed in the Gulf of Mexico, the North Sea, in Oman, and in the U.K. by Shell and British Petroleum (BP) [3].

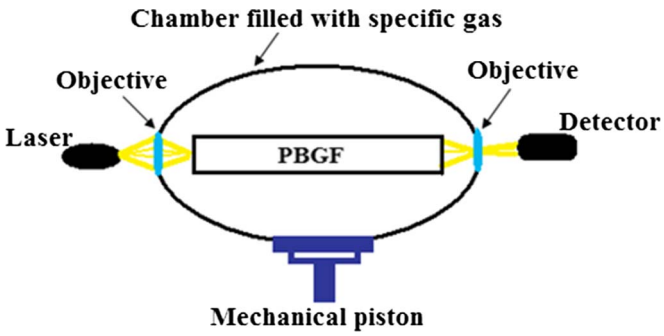

Fig. 1. Schematic of the proposed design of the PCF sensor.

Most pressure sensors using conventional optical fibers require that pressure be converted into another parameter before being transformed into an optical measurand [5]. In diaphragm-based Fabry–Perot (FP) interferometric fiber pressure sensor, a tiny FP cavity is fabricated at the tip of the fiber, and the pressure can be monitored from the reflected beam intensity [6], [7]. In some other sensors, fiber Bragg grating has been used [3]. Pressure variation changes the Bragg grating period, which causes wavelength shift of the reflected light that can be measured. In all cases, complex mechanical and optical apparatus are needed, sensitivity to pressure is low, and sensitivity to temperature is a challenging issue where compensation techniques are required.

In recent years, photonic crystal fibers (PCFs) have emerged, in which propagation conditions are realized by a set of holes regularly distributed around the solid core or light is guided in a hollow core surrounded by a cladding structure [8]. This kind of fibers has a wide potential in sensing applications. Its special structure with flexible design opens new opportunities for exploiting overlap between air holes and field of guiding mode in the core and somewhat in clad. So, we can observe that guiding light affects air hole properties such as geometry and refractive index. Another remarkable advantage of these PCF-based sensors is their low temperature dependence when they are used as pressure sensors [8].

In 2003, Hoo *et al.* proposed a designed gas PCF sensor containing the target gas in the holes with a length of few centimeters in which the response time of the PCF determines the target gas [9],

In 2006, Bock *et al.* reported a pressure sensor using PCF exposed to pressure changes externally with low sensitivity, in which pressure changes affect the polarization of the transmitting light [10]. Olivia *et al.* in 2009 presented a PCF pressure sensor using different mechanisms to enhance the sensitivity in which pressure affects the sensing directly by filling the holes [11]. Using PCF in this method and coiling it circularly make the PCF pressure and temperature sensor more sensitive and practical with nearly 3.24-nm/Mpa sensitivity [4].

In this paper, we propose a new design of sensor based on a hollow-core PCF for measuring pressure and temperature in the hostile environment of the oil wells. Our research is based on numerical analysis method. The validation of the proposed design is carried out by employing a 3-D finite-difference time domain (FDTD) method with perfectly matched layers. The sensing mechanism in our design is based on the wavelength shift of the PCF resonance associated with the refractive index change induced by the gas sample that is affected by temperature/pressure changes, with special emphasis on geometric parameters of the PCF structure. Considering the findings of previous studies in this area [12], here, we present the new structure of PCF-based sensor. To our knowledge, as compared to the previously reported pressure sensors [4], [12], the proposed design for PCF has the highest sensitivity with a linear dependence of the resonance wavelength on the refractive index of the ambient and holes of PCF.

2. Design and Operation of Sensor

A 2-D schematic of our proposed sensor structure is demonstrated in Fig. 1. In the proposed design of sensor, hollow-core triangular PCF is located in a chamber. The chamber is filled with a fixed

amount of a specific gas. Light beam with TE polarization is coupled from a laser through the microscopic objective lens into the hollow-core PCF. At the end of chamber, TE-polarized light transmitting through the hollow-core PCF is collected by a microscope objective lens. The residual TM-polarized light can be removed by a linear polarizer.

The gas used in the chamber should have enough stability at high temperature of oil well without chemical reaction with materials used in the device (for example, noble gases such as argon). Another important point that should be taken into account is that the wall effect of the gas molecules must be as low as possible.

Principle specification of this design is realized by a mechanical piston. When we are using the sensor as a pressure sensor, the piston can move due to pressure of oil well environment. This causes the chamber gas to be compressed in high pressure or be dispersed in low pressure. The refractive index alternation of chamber gas caused by pressure/temperature change influences the refractive index of holes and consequently leads to variation of photonic band gap and fundamental modes of PCF. The change of refractive index affects the propagating light. So, we can measure the shift of transmission peak wavelength and, therefore, the corresponding pressure/temperature.

We define the sensitivity as the shift of peak wavelength versus the refractive index change of the gas, which fills the holes and surrounds the fiber. Following [12], we define the sensitivity as

$$S = \frac{\Delta\lambda_P}{\Delta n} \tag{1}$$

where $\Delta\lambda_P$ is the shift of peak wavelength in (m), and Δn is the refractive index changes in RIU.

This process can also be used for measuring the temperature. In this case, instead of pressure, the temperature causes the change in the refractive index of PCF holes. It should be noted that the piston is fixed when temperature is the measurand. Moreover, the sensor design has the ability to measure the pressure and temperature of different gases and liquids with no vacuum system.

To take the advantages of PCF, most of the mode energy should propagate in hollow cores, which are filled with gas. In our pressure sensor design, the thermooptic effect in the glass is much lower than the overall pressure sensitivity. However, temperature effect can be removed completely in pressure sensor by choosing a proper gas. In other word, if thermooptic coefficients in gas and in silica have opposite signs, this gives the possibility to compensate the temperature effect by properly tuning the distribution of mode energy between the air core and the glass cladding [8].

An important merit of the gas is its ability to be compressed much larger than liquids, which results in higher change of refractive index. The refractive index of a gas is a function of pressure, temperature, wavelength, and density. Selection of the proper gas requires experimental tests to know the change of refractive index of the gas in pressure and temperature range of the oil well. The piston of the design makes a chance to transform the pressure range of the oil well to the best range of pressure, which in PCF has the most sensitivity. So, basic limit for choosing a proper gas is determined by the temperature of the oil well. There are many references for the refractive indices of various gases in different conditions [13]–[16], but very limited data [like the International Association for the Properties of Water and Steam (IAPWS)] [15] are available at high temperature condition of oil well. In the proposed design, the variations of pressure and temperature are measured by the change of output optical wavelength resonance affected by the variation of refractive index of PCF sensor, and based on that, we analyze the sensitivity of the PCF versus the change of refractive index.

3. Results and Discussion

Our analysis is carried out by employing FDTD method with perfectly matched layers. The FDTD approach is based on a direct numerical solution of the time-dependent Maxwell equations. The method enables us for the effective and powerful simulation and analysis of even submicron devices with very fine structural details.

Typically tens centimeters long PCF down to few millimeters can be used as the sensor sited in the chamber. We ignore the loss of the PCF because of its short length and the optical nonlinearity

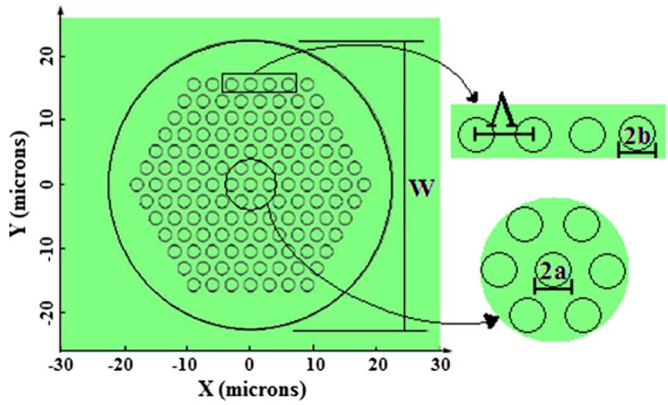

Fig. 2. Cross section of a PCF in XY plane, $a = b = 1$ μm, $N = 7$, $\Lambda = 3$ μm, $L = 1.8$ μm, and $W = 45$ μm.

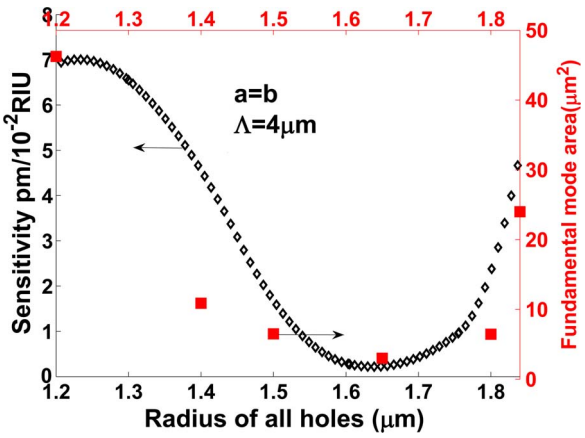

Fig. 3. Effect of holes radii on sensitivity (left axis). Fundamental mode area (right axis), for a PCF with $L = 1.8$ μm, $W = 90$ μm, $N = 7$, and $\Lambda = 4$ μm.

effects due to the using of low power laser. In our calculation, we consider a fixed value of refractive index for the silica part of the PCF because its refractive index sensitivity is about two orders of magnitude lower than the gas sensitivity.

The simulation has been done for a short-length PCF of 1.8 μm with the aim of analyzing geometric parameters of PCF and wavelength effects on its sensitivity. Regarding Fig. 2, which shows the cross section of a PCF, geometric parameters include pitch (Λ), radii of holes (b), radius of central hole (a), number of rings (N), and fiber's length (L) and diameter (W). In the analysis, the refractive index of holes and environment of the PCF, which is filled with gas, is changed around $n_0 = 1$ (the refractive index of vacuum) simultaneously to see the effect of outside temperature and pressure variation.

We use a continuous light source at 1.55 μm with a Gaussian field in the simulations. PCF sensitivity (S) is proportional to the overlap of the field with the holes containing the gas. Fig. 3 shows the effect of holes radii on sensitivity (left axis) and area of fundamental mode (right axis), for a PCF with $L = 1.8$ μm, $\Lambda = 4$ μm, $W = 90$ μm, and $N = 7$. Sensitivity has been defined as peak wavelength shift versus the refractive index change of ambient and holes of the PCF. Fundamental mode area is defined as the specified circular region in which the integrated power is about 80% of total guided power at the fundamental mode. Filled squares illustrate the area of fundamental mode for a PCF length of 1.8 μm and the nonfilled squares curve shows the sensitivity in pm$/10^{-2}$ RIU.

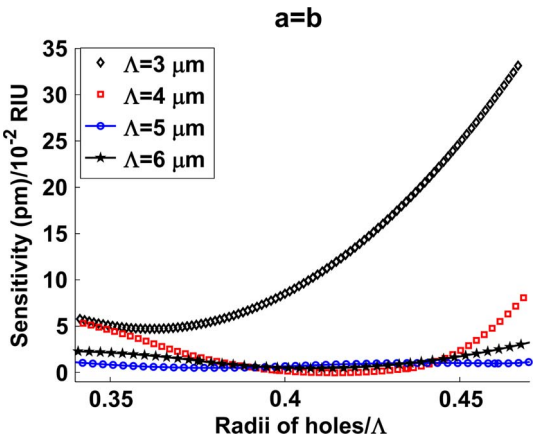

Fig. 4. Sensitivity versus radii of holes/pitch for different pitches (3, 4, 5 and 6 μm), $L = 1.8$ μm, $W = 15 \times \Lambda$, and $N = 7$.

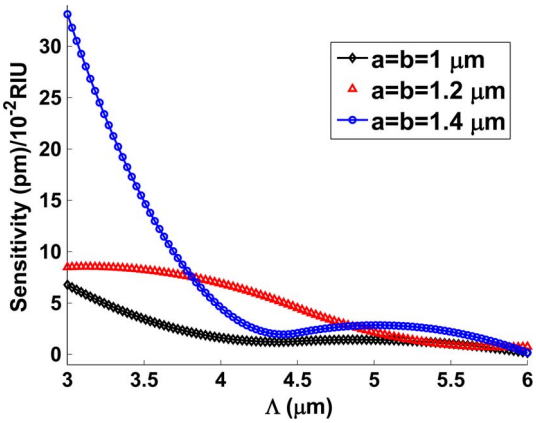

Fig. 5. Sensitivity versus the amount of pitch with $a = b = 1, 1.2, 1.4$ μm ($N = 7$, $L = 1.8$ μm, and $W = 15 \times \Lambda$).

By increasing holes radii, area of fundamental mode and the energy density of the electromagnetic field within the structure changes nonuniformly, which leads to the variation of sensitivity. By suitable design, these enhanced local fields increase the light-matter interaction. This consequently results in increasing overlap between fundamental mode and the refractive index of the gas, and thereby, sensitivity (which is proportional to the energy fraction of the resonant mode field interacting with the gas) increases.

Fig. 4 demonstrates the sensitivity as a function of radius of holes for different values of pitch $\Lambda = 3, 4, 5$, and 6 μm, and $a = b$. It can be seen that shorter pitches (3 and 4 μm) are followed by higher sensitivity and larger change of the sensitivity curves. This implies that the sensitivity at shorter pitches is strongly dependent on gas area. It should be noted that, in longer pitches (5 and 6 μm), the mode area plays a significant role in contrast to shorter pitches.

In Fig. 5, the sensitivity is plotted for different values of pitch while radii of holes are fixed. As we expect, increasing the hole size and decreasing the amount of pitch have the same effect on the sensitivity because, in both cases, the gas area increases. For higher pitch values (as $\Lambda = 5, 6$ μm), the sensor has lower sensitivity with a small variation versus radii of holes$/\Lambda$. The results show that we can reach the sensitivity of 33 pm/RIU by changing the pitch and holes radii. In other words, with a proper design, as the pitch value decreases the fraction of overlap between the gas filled area and

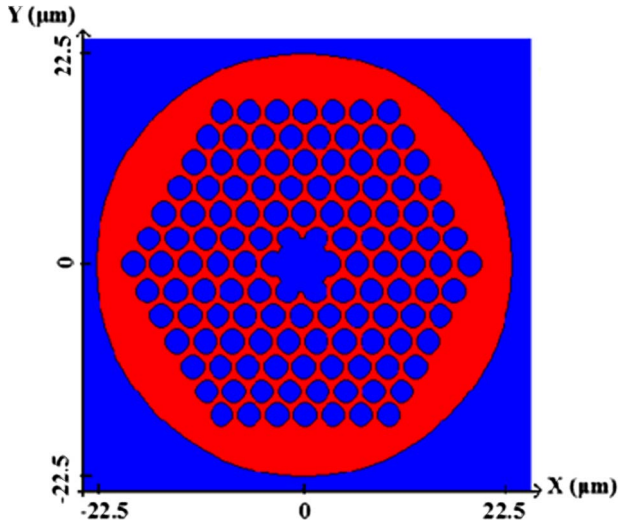

Fig. 6. Sample PCF: $L = 1.8\ \mu$m, $W = 45\ \mu$m, $N = 7$, $\Lambda = 3\ \mu$m, $a = 2\ \mu$m, and $b = 1.4\ \mu$m.

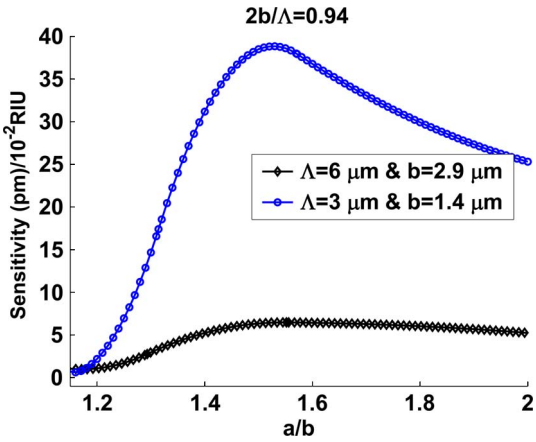

Fig. 7. Effect of central hole radius change on sensitivity for two different pitches (3 and 6 μm), while the ratio of radius of others holes to the amount of pitch is 0.94 ($L = 1.8\ \mu$m, $W = 15 \times \Lambda$, and $N = 7$).

the fundamental mode area will be increased, which causes the increment in the amount of sensitivity, and the same phenomenon happens as the hole size increases.

Since the central hole in the PCF has an important role on sensitivity by overlapping with the mode area, we analyze its geometric effect on sensitivity. With increment of central hole radius more than length of pitch, there will be an overlap between the central hole and the adjacent holes as shown in Fig. 6. In Fig. 7, the effect of central hole radius change on sensitivity is shown for two different pitches (3 and 6 μm) versus the ratio of radius of central hole to other holes (a/b), while the ratio of radius of others holes to the pitch $(2b/\Lambda)$ is 0.94. That is, the maximum area of the PCF is occupied by the gas. We see that the sensitivity has a maximum amount of 35 pm/RIU around $a/b = 1.5$. Higher values of central hole radius causes the increase of sensitivity up to a maximum amount; however, beyond a specific value of a/b, the confinement of fundamental mode decreases, which leads to the drop of sensitivity as depicted in the figure.

In Fig. 8, sensitivity results for two other different PCF designs with $\Lambda = 3\ \mu$m versus the ratio of radius of central hole to other holes (a/b) are presented with the radius of central hole as a parameters. The sensitivity changes with b, and it has a greater maximum for larger values of b. For example, the sensitivity is about 37 and 22 pm$/10^{-2}$ RIU for $b = 1.4$ and 1 μm, respectively.

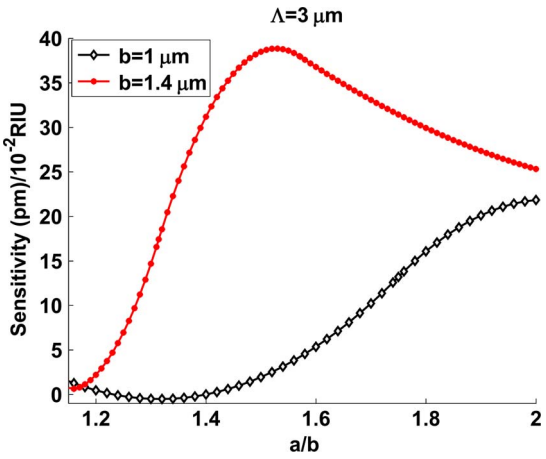

Fig. 8. Effect of central hole change on sensitivity for the same pitch (3 μm) versus $L = 1.8$ μm, $W = 45$ μm, and $N = 7$).

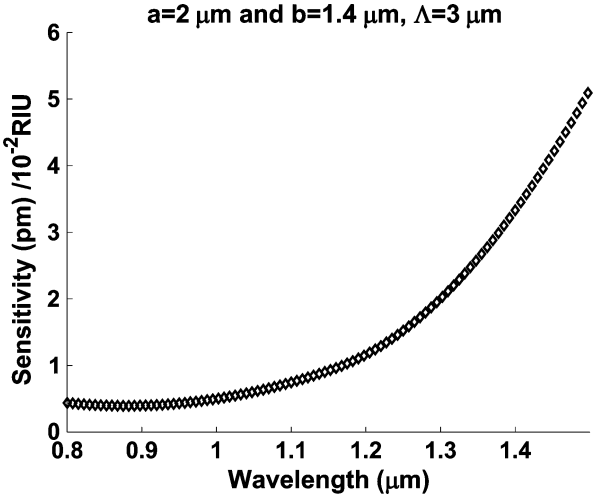

Fig. 9. Sensitivity versus wavelength for the PCF with $\Lambda = 3$ μm, $a = 2$ μm, $b = 1.4$ μm, $L = 1.8$ μm, $W = 90$ μm, and $N = 7$.

In Fig. 9, we analyze the sensitivity versus input optical wavelength for a PCF with $\Lambda = 3$ μm, $a = 2$ μm, $b = 1.4$ μm, $L = 1.8$ μm, $W = 90$ μm, and $N = 7$. Note that the group index in silica is inversely related to the wavelength of light [17], that is, lower group index for higher wavelengths (in our operating wavelength region); thus, it has the similar effect on sensitivity as increasing the hole size.

Fig. 10 shows the sensitivity at 1.55 μm versus the number of rings for a PCF with $L = 1.8$ μm, $W = 90$ μm, $\Lambda = 3$ μm, $a = 2$ μm, and $b = 1.4$ μm. Further rings results in more sensitivity. For higher number of rings, it has no considerable change because the light is confined and the fundamental mode area approximately has no change.

Fig. 11 shows the peak wavelength shift versus different polarizations of input light for the PCF with a high sensitivity around 3.5 nm/RIU with $L = 1.8$ μm, $N = 7$, $\Lambda = 3$ μm, $a = 2$ μm, and $b = 1.4$ μm. The slopes of the curves show the sensitivity. We see the higher sensitivity is for the right-hand circular polarization. So far, we have analyzed the PCF sensitivity for different structures, where we obtained the max sensitivity for the PCF with $L = 1.8$ μm, $W = 90$ μm, $N = 7$, $\Lambda = 3$ μm, $a = 2$ μm, and $b = 1.4$ μm.

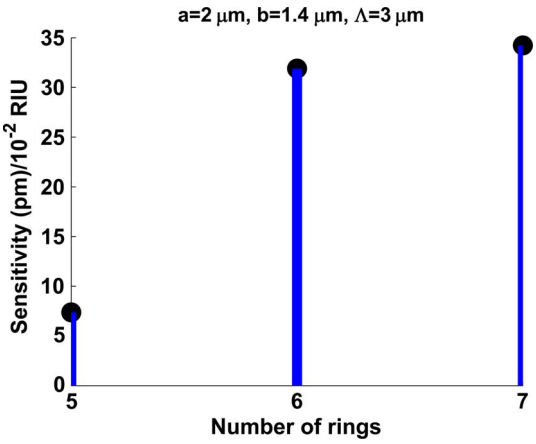

Fig. 10. Sensitivity versus number of ring for a PCF with $L = 1.8$ μm and $W = 90$ μm.

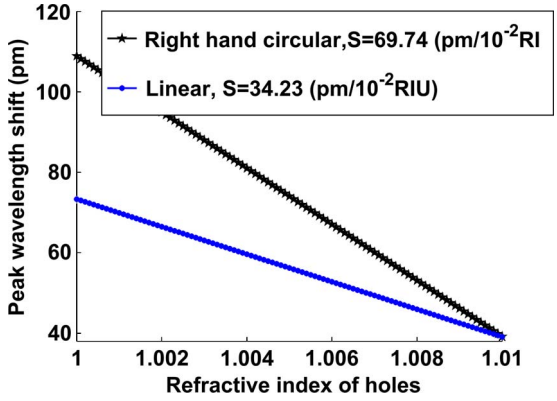

Fig. 11. Variation of peak wavelength as a function of holes refractive index with the polarization of input light as a parameter, for a PCF with ($L = 1.8$ μm, $W = 90$ μm, $N = 7$, $\Lambda = 3$ μm, $a = 2$ μm, and $b = 1.4$ μm).

The effect of light source polarization and wavelength on the sensitivity of this PCF is summarized in Table 1. The circular polarization of input light results in higher sensitivity as compared with the linear polarization.

All the simulation results were obtained for a PCF length of 1.8 μm, but practically, most sensors have longer lengths. Here, we use the optimized structure (with higher sensitivity) to analyze for longer length of the PCF to increase the sensitivity. So, we analyze the sensitivity for the PCF with specifications of Fig. 6 for a length of 250 μm at 1.55 μm and linear input polarization. We obtain a sensitivity of 483.22 nm/RIU. This short PCF decreases the response time of the sensor. In Table 2, we compare the sensitivity of our PCF sensor design with the others works. We have converted sensitivity of [3], [4], and [12] in Table 2 to the scale of nm/Mpa using [13]. This conversions is done for a typical gas (here propane) in which pressure change is converted to refractive index change at a fixed high temperature (about 120 °C), to make them comparable with each other. To our knowledge, the sensitivity that we obtained here by the proposed design of PCF sensor is much higher than other sensors reported so far.

4. Conclusion

We proposed a new design of pressure/temperature PCF sensor and analyzed the effects of geometrical parameters on PCF sensitivity. Sensitivity has been defined as peak wavelength shift

TABLE 1

Effect of light source polarization and wavelength on the sensitivity for the PCFs with $L = 1.8$ μm, $W = 90$ μm, $N = 7$, $\Lambda = 3$ μm, $a = 2$ μm, and $b = 1.4$ μm

Sensitivity	Polarization	Wavelength (μm)
34.23 Pm/10^{-2} RIU	linear	1.55
0.5 Pm/10^{-2} RIU	linear	1.3
69.74 Pm/10^{-2} RIU	Right hand circular	1.55

TABLE 2

Comparison of proposed design with the other practical works

Sensitivity nm/Mpa	Sensor	Year	Reference
0.022	BGF	2006	[3]
20	PC	2008	[12]
3.24	PCF	2010	[4]
120.75	PCF	2011	Our design

versus the refractive index change of ambient and holes of the PCF. We see in a PCF with homogenous holes that the increase in hole size results in higher sensitivity if the fundamental mode area increases. We studied the effect of radii of holes and the amount of pitch on the sensitivity of the PCF. The effect of light source polarization and the wavelength on the sensitivity of the PCF has been studied. We obtained the sensitivity of about 480 nm/RIU for a 0.25-mm length of our proposed PCF sensor, which is, to our knowledge, much higher than other sensors reported so far.

References

[1] E. L. E. Kluth, M. P. Varnham, J. R. Clowes, R. L. Kutlik, C. M. Crawley, and R. F. Heming, "Advanced sensor infrastructure for real time reservoir monitoring," in *Proc. SPE Eur. Petroleum Conf.*, Paris, France, 2000, pp. 24–25.

[2] T. K. Kragas, B. A. Williams, and G. A. Myers, "The optic oil field: Deployment and application of permanent in-well fiber optic sensing systems for production and reservoir monitoring," presented at the SPE Annu. Tech. Conf. Exhibition, New Orleans, LA, 2001.

[3] S. H. Aref, H. Latifi, M. I. Zibaii, and M. Afshari, "Fiber optic Fabry–Perot pressure sensor with low sensitivity to temperature changes for downhole application," *Opt. Commun.*, vol. 269, no. 2, pp. 322–330, Jan. 2007.

[4] H. Y. Fu, C. Wu, M. L. V. Tse, L. Zhang, K. D. Cheng, H. Y. Tam, B. Guan, and C. Lu, "High pressure sensor based on photonic crystal fiber for downhole application," *J. Appl. Opt.*, vol. 49, no. 14, pp. 2639–2643, May 2010.

[5] K. Fidanboylu and H. S. Efendioglu, "Fiber optic sensors and their applications," in *Proc. 5th IATS*, Karabuk, Turkey, 2009.

[6] P. C. Beard and T. N. Mills, "Miniature optical fiber ultrasonic hydrophone using a Fabry–Perot polymer film interferometer," *Electron. Lett.*, vol. 33, no. 9, pp. 801–803, Apr. 1997.

[7] H. Dooyoung, Y. Euisik, and H. Songcheol, "An optomechanical pressure sensor using multimode interface couplers," *Jpn. J. Appl. Phys.*, vol. 38, no. 4B, pp. 2664–2668, Apr. 1999.

[8] T. Nasilowski, F. Berghmans, T. Geernaert, K. Chah, J. Van Erps, G. Statkiewicz, M. Szpulak, J. Olszewski, G. Golojuch, T. Martynkien, W. Urbanczyk, P. Mergo, M. Makara, J. Wojcik, C. Chojetzki, and H. Thienpont, "Sensing with photonic crystal fibers," in *Proc. Intell. Signal Process.*, 2007, pp. 1–6.

[9] Y. L. Hoo, W. Jin, C. Shi, H. L. Ho, D. N. Wang, and S. C. Ruan, "Design and modeling of a photonic crystal fiber gas sensor," *J. Appl. Opt.*, vol. 42, no. 18, pp. 3509–3515, Jun. 2003.

[10] W. J. Bock, J. Chen, T. Eftimov, and W. Urbanczyk, "A photonic crystal fiber sensor for pressure measurements," *IEEE Trans. Instrum. Meas.*, vol. 55, no. 4, pp. 1119–1123, Aug. 2006.

[11] R. E. P. D. Oliveria, C. J. D. Matos, J. G. Hayashi, and C. M. B. Corderio, "Pressure sensing based on nonconventional air-guiding transmission windows in hollow-core photonic crystal fibers," *J. Lightw. Technol.*, vol. 27, no. 11, pp. 1605–1609, Jun. 2009.

[12] T. Sunner, T. Stichel, S. H. Kwan, T. W. Schlereth, S. Hofling, M. Kamp, and A. Forchel, "Photonic crystal cavity based gas sensor," *Appl. Phys. Lett.*, vol. 92, no. 26, pp. 261112-1–261112-3, Jun. 2008.

[13] J. Hadrich, "The Lorentz–Lorenz function of five gaseous and liquid saturated hydrocarbons," *Appl. Phys. A*, vol. 7, no. 3, pp. 209–213, Jul. 1975.
[14] J. A. McCaulley, V. M. Donnelly, M. Vernon, and I. Taha, "Temperature dependence of the near infrared refractive index of silicon gallium arsenide and indium phosphide," *J. Phys. Rev. B*, vol. 49, no. 11, pp. 7408–7417, Mar. 1994.
[15] P. E. Ciddor, "Refractive index of air: New equations for the visible and near infrared," *Appl. Optics*, vol. 35, no. 9, pp. 1566–1573, Mar. 1996.
[16] R. Fernandez-Prini and R. B. Dooley, "Release on the refractive index of ordinary water substance as a function of wavelength, temperature and pressure," in *Proc. Int. Assoc. Properties Water Steam*, Erlangen, Germany, 1997.
[17] G. P. Agrawal, *Nonlinear Fiber Optics*. Amsterdam, The Netherlands: Elsevier, 2007.